Lattice-gas simulations of domain growth, saturation, and self-assembly in immiscible fluids and microemulsions

Andrew N. Emerton*
Department of Theoretical Physics, Oxford University, 1 Keble Road, Oxford OX1 3NP, United Kingdom

Peter V. Coveney†
Schlumberger Cambridge Research, High Cross, Madingley Road, Cambridge CB3 0EL, United Kingdom

Bruce M. Boghosian‡
Center for Computational Science, Boston University, 3 Cummington Street, Boston, Massachusetts 02215
(Received 12 March 1996; revised manuscript received 16 September 1996)

We investigate the growth kinetics of both binary fluid and ternary microemulsion systems in two dimensions using a recently introduced hydrodynamic lattice-gas automaton model of microemulsions. We find that the presence of amphiphile in our simulations reduces the usual oil-water interfacial tension in accord with experiment and consequently affects the nonequilibrium growth of the oil and water domains. As the density of surfactant is increased we observe a crossover from the usual two-dimensional binary fluid scaling laws to a growth that is *slow*, and we find that, up to a point, this slow growth can be characterized by a logarithmic time scale. With sufficient surfactant in the system we observe that the domains cease to grow beyond a certain point; we find that this final characteristic domain size is inversely proportional to the interfacial surfactant concentration in the system and that a stretched-exponential functional form accurately describes the data across the whole time scale of the simulations in these cases. [S1063-651X(97)08101-4]

PACS number(s): 82.70.−y

I. INTRODUCTION

The introduction of amphiphilic molecules into a system of oil and water is known to have marked effects on the properties and behavior of such mixtures. As a result of the particular physical and chemical properties of surfactant molecules one can observe the formation of a wealth of complex structures. For a general review see Gelbart *et al* [1]. One major feature of these systems is that the usual oil-water interfacial tension is dramatically lowered by the presence of amphiphile [2], this being the origin of much of the commercial interest in such self-assembling structures. Making use of the dynamical nature of our recently introduced hydrodynamic lattice-gas model of microemulsions [3], we demonstrate that it is able to consistently simulate this important experimentally observed phenomenon.

Growth kinetics in binary immiscible fluids have received much attention recently. Phase separation in these systems has been simulated using a variety of techniques: these include cell dynamical systems without hydrodynamics [4] and with Oseen tensor hydrodynamics [5]; time-dependent Ginzburg-Landau models without hydrodynamics [6], and with hydrodynamics [7–9]; as well as lattice-gas automata [10,11] and the related lattice-Boltzmann techniques [12]. A central quantity in the study of growth kinetics is the time-dependent average domain size $R(t)$. For binary systems in the regime of sharp domain walls, this follows algebraic growth laws of the form $R(t)\sim t^n$. In general, previous simulations have confirmed experimental observations and theoretical predictions [13,14] for these systems. That is, for models without hydrodynamic interactions (binary alloys) the growth exponent is found to be $n=\frac{1}{3}$, independent of the spatial dimension. If flow effects are relevant (binary fluids), and the domain size R is greater than the hydrodynamic length $R_h=(\nu^2/\rho\sigma)$ [13], where ν is the kinematic viscosity, ρ is the density, and σ is the surface tension coefficient, then one obtains $n=\frac{2}{3}$ in two space dimensions. We use our lattice-gas model to investigate this as well as the less commonly observed $R<R_h$ regime in two-dimensions (2D), which has not been accessed before with lattice gases; this is described in Sec. IV. In three dimensions in the regime $R<R_h$ the growth exponent is $n=\frac{1}{3}$ crossing over to $n=1$ at late times, with $n=\frac{2}{3}$ if $R>R_h$.

The lowering of the oil-water interfacial tension by amphiphile has important consequences for the nonequilibrium dynamical growth of domains within ternary systems. Our microscopic lattice-gas model of microemulsions, which correctly models the mesoscopic and macroscopic fluid behavior, enables us to investigate such dynamical domain growth. In ternary systems, growth kinetics has previously been studied by numerical integration of time-dependent Ginzburg-Landau models, for example, the hybrid models of Kawakatsu *et al.* [15] and the two local order parameter model of Laradji *et al.* [16,17]. These models do not include hydrodynamic effects and find that surfactants modify the dynamics from the binary $n=\frac{1}{3}$ algebraic exponent to a slow growth that may be logarithmic in time. More recently Laradji *et al.* [18] have modeled phase separation in the presence of surfactants using a very simple molecular dynamics

*Electronic address: emerton@thphys.ox.ac.uk
†Electronic address: coveney@cambridge.scr.slb.com
‡Electronic address: bruceb@bu.edu

model which implicitly includes hydrodynamic forces. These authors found that such systems exhibit nonalgebraic, slow growth dynamics and that the average domain size saturates at a value inversely proportional to the surfactant concentration. They also found a crossover scaling form which describes the change from the algebraic growth in pure binary fluids to a slower domain growth when surfactants are present. This scaling Ansatz was observed to hold with an exponent $n=1/2$, which corresponds to the binary growth exponent seen at intermediate times in 2D in other recent simulations, as discussed in Sec. IV. Contrasting with these results, Pätzold and Dawson [19] have recently suggested that with noise included in a time-dependent hydrodynamic Ginzburg-Landau model, binary-fluid-like power-law growth behavior can be observed across the whole range of surfactant densities, with the exponent decreasing as the amount of surfactant is increased. However, this is clearly not how real microemulsion systems behave: Even with noise present in the system, one would expect domain growth to cease once sufficient surfactant is present, and consequently one would also expect the growth to slow down significantly prior to this. We believe that the technique employed by Pätzold and Dawson has not allowed them to access the true late-time dynamics with noise present in the system; although this may simply be due to them choosing to do fits using effective exponents rather than probing other growth laws and due to the fact that the scaling region within which they calculated the exponents is probably too short for intermediate to high surfactant concentrations. Access to this asymptotic regime is also difficult for molecular dynamics simulations. Lattice-gas automaton models, on the other hand, while including by construction the correct hydrodynamics, permit simulations over a wider range of relevant time scales than those techniques described above. Fluctuations are an inherent and important physical component of such models, and consequently our microemulsion model provides useful and arguably unique insight into the dynamics of such complex systems.

Characterization of the slow growth found in these amphiphilic systems prior to saturation of the domain size remains a challenge. Comparative slowing down in domain growth has been observed in 2D simulations of systems with quenched impurities [20], where the growth is described by a logarithmically slow activated process with $R(t)\sim(\ln t)^{\theta}$. For these systems the surface tension diminishes over time, whereas for amphiphilic systems, which may not be quenched in the same sense as the impurities in these models, the surface tension begins to be affected as soon as the molecules reach oil-water interfaces. Here we are interested in the growth laws that are observed as we approach the ''saturation'' point in our system. This is the point at which self-similarity and the usual scaling laws must break down: In some sense there must be an exponential tailoff in the growth of domain size as the saturation point is reached. The results obtained using our microemulsion model for domain growth in these ternary systems as the quantity of surfactant is varied are presented in Sec. V.

The purpose of this paper is to establish that our lattice-gas automaton amphiphilic model exhibits the correct physical and kinetic behavior in both the binary and ternary phases, as well as extending what is currently known about these models and systems with reference to certain specific areas. Section II contains a brief review of our lattice-gas model. In Sec. III we use the dynamical nature of our model in order to make a direct numerical evaluation of the oil-water interfacial tension both with and without surfactant present. The determined reduction of the interfacial tension in the former case, which is our result for dynamical lattice-based models and can be more closely compared with experimental results than other models, has a direct effect on the growth kinetics of domains which we subsequently investigate in Secs. IV and V. In the latter ternary microemulsion case, we detail the slow domain growth observed and find that a stretched-exponential functional form is the best fit to the data when saturation of the system occurs.

II. THE LATTICE-GAS AUTOMATON MODEL

Our lattice-gas model is based on a microscopic particulate format that allows us to include dipolar surfactant molecules alongside the basic oil and water particles [3]. In this paper we are only concerned with a two-dimensional version of the model, though an extension to the three-dimensional version (3D) is currently underway [21]. Working on a triangular lattice with lattice vectors $\mathbf{c}_i$ $(i=1,\ldots,6)$, the state of the 2D model at site $\mathbf{x}$ and time t is completely specified by the occupation numbers $n_i^{\alpha}(\mathbf{x},t)\in\{0,1\}$ for particles of species α and velocity $(\mathbf{c}_i/\Delta t)$.

The evolution of the lattice gas for one time step takes place in two substeps. In the *propagation* substep the particles simply move along their corresponding lattice vectors. In the *collision* substep the newly arrived particles change their state in a manner that conserves the mass of each species as well as the total D-dimensional momentum.

We allow for two immiscible species which, following convention, we often represent by colors: $\alpha=B$ (blue) for water, and $\alpha=R$ (red) for oil, and we define the *color charge* of a particle moving in direction i at position $\mathbf{x}$ at time t as $q_i(\mathbf{x},t)\equiv n_i^R(\mathbf{x},t)-n_i^B(\mathbf{x},t)$. Interaction energies between outgoing particles and the total color charge at neighboring sites can then be calculated by assuming that a color charge induces a *color potential* $\phi(r)=qf(r)$, at a distance r away from it, where $f(r)$ is some function defining the type and strength of the potential.

To extend this model to amphiphilic systems, we also introduce a third (surfactant) species S, and the associated occupation number $n_i^S(\mathbf{x},t)$, to represent the presence or absence of a surfactant particle. Pursuing the electrostatic analogy, the surfactant particles, which generally consist of a hydrophilic portion attached to a hydrophobic (hydrocarbon) portion, are modeled as *color dipole vectors*, $\boldsymbol{\sigma}_i(\mathbf{x},t)$. As a result, the three-component model includes three additional interaction terms, namely, the color-dipolar field, the dipole-color field, and the dipole-dipole interactions.

The total interaction energy that results can be written

$$\begin{aligned}\Delta H_{\mathrm{int}}&=\Delta H_{\mathrm{cc}}+\Delta H_{\mathrm{cd}}+\Delta H_{\mathrm{dc}}+\Delta H_{\mathrm{dd}}\\&=\left[\left(\mathbf{J}+\frac{\boldsymbol{\sigma}'}{\Delta t}\right)\cdot(\mathbf{E}+\mathbf{P})+\mathcal{J}:(\mathcal{E}+\mathcal{P})\right]\Delta t,\end{aligned}\tag{1}$$

where we have defined the *color flux* of an outgoing state

$$\mathbf{J}(\mathbf{x},t)\equiv\sum_{i}^{n}\frac{\mathbf{c}_i}{\Delta t}q_i'(\mathbf{x},t) \tag{2}$$

(the sum extending over all lattice vectors at a site, so that in this case $n=6$), and the *color field*

$$\mathbf{E}(\mathbf{x},t)\equiv\sum_{\mathbf{y}\in\mathcal{L}}f_1(y)\mathbf{y}q(\mathbf{x}+\mathbf{y},t), \tag{3}$$

where the sum is over sites $\mathbf{y}$ which are elements of the hexagonal lattice $\mathcal{L}$. For short-range forces, the function f_1 has compact support so that this sum includes only sites nearby $\mathbf{x}$. The *dipolar field* vector is

$$\mathbf{P}(\mathbf{x},t)\equiv-\sum_{\mathbf{y}\in\mathcal{L}}[f_2(y)\mathbf{y}\mathbf{y}-f_1(y)\mathbf{1}]\cdot\boldsymbol{\sigma}(\mathbf{x}+\mathbf{y},t), \tag{4}$$

where $\mathbf{1}$ denotes the rank-two unit tensor and $\boldsymbol{\sigma}'\equiv\Sigma_i\boldsymbol{\sigma}_i$ represents the total outgoing dipolar vector at a site. Similarly we have defined the *dipolar flux tensor*

$$\mathcal{J}(\mathbf{x},t)\equiv\sum_{i}^{n}\frac{\mathbf{c}_i}{\Delta t}\boldsymbol{\sigma}_i'(\mathbf{x},t), \tag{5}$$

and the *color-field gradient tensor*

$$\mathcal{E}(\mathbf{x},t)\equiv\sum_{\mathbf{y}\in\mathcal{L}}q(\mathbf{x}+\mathbf{y},t)[f_2(y)\mathbf{y}\mathbf{y}-f_1(y)\mathbf{1}], \tag{6}$$

where again $\mathbf{1}$ denotes the rank-two unit tensor. Finally we have the *dipolar field gradient* tensor

$$\mathcal{P}(\mathbf{x},t)=-\sum_{\mathbf{y}\in\mathcal{L}}\boldsymbol{\sigma}(\mathbf{x}+\mathbf{y},t)\cdot[f_3(y)\mathbf{y}\mathbf{y}\mathbf{y}-f_2(y)\mathbf{y}\cdot\boldsymbol{\Omega}], \tag{7}$$

wherein $\boldsymbol{\Omega}$ is the completely symmetric and isotropic fourth-rank tensor. In Eqs. (3), (4), (6), and (7) we have defined certain derivatives of the function $f(r)$

$$f_{\ell}(y)\equiv\left(-\frac{1}{y}\frac{d}{dy}\right)^{\ell}f(y), \tag{8}$$

where ℓ is a positive integer or zero [3].

The collision process of the algorithm consists of enumerating the outgoing states allowed by the conservation laws, calculating the total interaction energy for each of these, and then, following the ideas of Chan and Liang [22] (see also Chen *et al.* [23]), forming Boltzmann weights

$$e^{-\beta\Delta H}, \tag{9}$$

where β is an inverse temperaturelike parameter. The postcollisional outgoing state and dipolar orientations can then be obtained by sampling from the probability distribution formed from these Boltzmann weights; consequently the update is a stochastic process. The dipolar orientation streams with surfactant particles in the usual way.

Our model's parameter space has certain important pairwise limits. With no surfactant in the system, Eq. (1) reduces to the color-color interaction term only,

$$\Delta H_{\mathrm{cc}}\equiv\mathbf{J}\cdot\mathbf{E},$$

which we note to be exactly identical to the expression for the total color work used by Rothman and Keller [24] to model immiscible fluids. Correspondingly, with no oil in the system we are free to investigate the formation and dynamics of the structures that are known to form in binary water-surfactant solutions. Indeed, in our original paper [3] we investigated both of these limits. In the limit of no surfactant we obtained immiscible fluid behavior similar to that observed by Rothman and Keller, and for the case of no oil in the system we found evidence for the existence of micelles and for a critical micelle concentration. Moreover, we demonstrated that this model exhibits the correct 2D equilibrium microemulsion phenomenology for both binary and ternary phase systems using a combination of visual and analytic techniques; various experimentally observed self-assembling structures, such as the droplet and bicontinuous microemulsion phases, form in a consistent manner as a result of adjusting the relative amounts of oil, water and amphiphile in the system. The presence of enough surfactant in the system is shown to halt the expected phase separation of oil and water, and this is achieved without altering the coupling constants from values that produce immiscible behavior in the case of no surfactant.

Note that in order to incorporate the most general form of interaction energy within our model system, we introduce a set of coupling constants $\alpha,\mu,\epsilon,\zeta$, in terms of which the total interaction energy can be written as

$$\Delta H_{\mathrm{int}}=\alpha\Delta H_{\mathrm{cc}}+\mu\Delta H_{\mathrm{cd}}+\epsilon\Delta H_{\mathrm{dc}}+\zeta\Delta H_{\mathrm{dd}}. \tag{10}$$

These terms correspond, respectively, to the relative immiscibility of oil and water, the tendency of surrounding dipoles to bend around oil or water particles and clusters, the propensity of surfactant molecules to align across oil-water interfaces, and a contribution from pairwise (alignment) interactions between surfactants. In the present paper we analyze domain growth of critical quenches within both binary and ternary systems and consequently the two coefficients with which we are most concerned are α and ϵ.

III. SURFACE TENSION ANALYSIS

The lowering of the interfacial tension between oil and water by the action of surfactant molecules located at such interfaces is an important property of microemulsions. Experimental investigation of polymer–block-copolymer systems, where the time scales are much slower than in the related microemulsions, has made studies of such characteristics possible [25]. In the present section, we analyze the surface tension within a system of oil, water, and surfactant as it varies with the surfactant density (concentration). We work with $\beta=1.0$ and use, consistently throughout this paper, $\alpha=1.0$, $\mu=0.001$, $\epsilon=8.0$, $\zeta=0.005$ as the values of the coefficients in Eq. (10), strongly encouraging surfactant molecules to accumulate at oil-water interfaces while maintaining the normal oil-water immiscible behavior.

We begin by showing that our model, in the limiting case of two immiscible fluids, produces physically realistic interfacial tensions. In terms of the basic two-species Rothman-Keller immiscible lattice-gas, surface tension has been extensively investigated from both a theoretical and a numerical viewpoint by Adler, d'Humières, and Rothman [26]. Using a

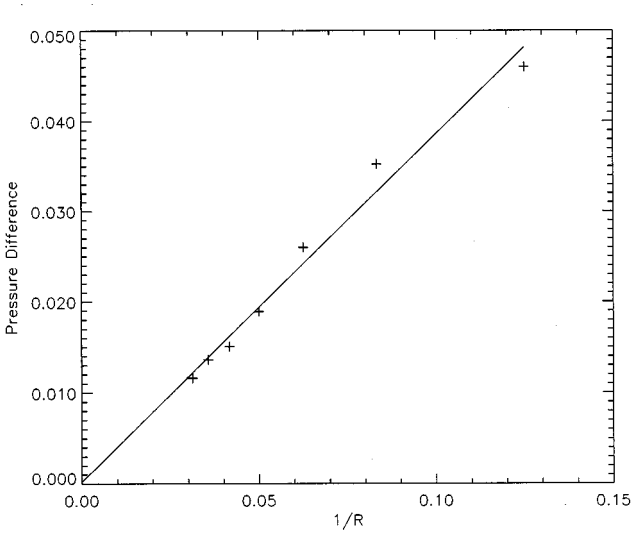

FIG. 1. Verification of Laplace's law and estimation of surface tension for two immiscible fluids (oil and water) only.

bubble experiment as described in their paper, we can check the validity of our basic model by evaluating the surface tension in the immiscible fluid case. We use Laplace's law, which in two dimensions is

$$P_{\text{in}} - P_{\text{out}} = \frac{\sigma}{R}, \tag{11}$$

where σ is the oil-water interfacial tension, R is the radius of the bubble, P_{in} is the average pressure within the bubble, and P_{out} the average pressure outside. Simulations are carried out using bubbles with a number of different radii. The pressure in lattice gases is given in tensorial form by [27]

$$P_{\alpha\beta} = \sum_{i=0}^{6} c_{i\alpha} c_{i\beta} N_i, \tag{12}$$

where α and β are tensor indices, and the expression can be evaluated by calculating the distribution of the populations N_i. The pressure arises as a result of the collision step of the lattice dynamics and so to a good approximation is dependent on local interactions only. The results from our simulations are shown in Fig. 1. They give good agreement with Laplace's law, and a best-fitting line through the origin results in an estimate of $\sigma \approx 0.378$, close to the results reported by Adler and co-workers [26].

We now turn to the analysis of the interfacial tension for varying initial concentrations of surfactant in the system, where in each case the amphiphile is added at an initially flat, bulk oil-water, interface. We make use of a direct dynamical method of calculating the surface tension across this flat interface, although, due to the complex dynamical nature of the microemulsion behavior we are modeling, as more surfactant is added we have to allow for progressively more extensive relaxation of the system before collecting data on the equilibrated system. For the case of a flat interface perpendicular to the z axis, the surface tension σ is given by the integral over z of the difference between the component P_N of pressure normal to the interface and the component P_T transverse to the interface [26,28]:

$$\sigma = \int_{-\infty}^{\infty} [P_N(z) - P_T(z)] dz. \tag{13}$$

This quantity can be calculated by empirically computing the given integral while remembering to take the underlying lattice into account. It is worth noting that no equilibrium microemulsion model can measure the surface tension this directly since the method is inherently dynamical; equilibrium models rely on calculating σ as a function of various *interaction parameters*. Indeed, the few other simulation models that do include dynamical effects for such complex fluids, often depend on the evolution of order parameters (for instance, time-dependent Ginzburg-Landau models) and as such have a coefficient that is simply tuned in order to alter the surface tension. There is an important caveat to be mentioned here: as the initial concentration of surfactant in the system is increased one finds that the initially stable oil-water interface begins to show signs of distortion and breakup. This effect arises as a result of the energetics of the system; preferentially surfactant particles reside in thin (mono)layers at oil-water surfaces and consequently the system acts to create as much oil-water interfacial length as possible in order to accommodate the amphiphile. At some critical density of surfactant it is clear that the initially flat interface will break up completely; indeed, we then see the formation of a bicontinuous ''middle'' phase corresponding to an effective oil-water surface tension of zero. At and beyond this point the methods outlined above for measuring σ are ineffective. However, below this critical density we expect to be able to use Eq. (13) to evaluate the surface tension, bearing in mind that, as we add more surfactant to the system, we have to wait correspondingly longer for the interface to relax before relevant measurements of $<n_i>$ can be made; we expect sections of negative values for σ prior to equilibration and denote these as being part of a ''transient region.'' In the asymptotic region the interface stabilizes and only positive average values for the surface tension are found; this is denoted as the ''smooth region.''

The results shown in Fig. 2 are the values of interfacial tension obtained, *once the smooth region has been reached*, for varying initial concentrations of surfactant in the system; the error bars from the subsequent time average are smaller than the size of the symbols and so are not included. The plotted values of surfactant density are given as a proportion of the total reduced density of oil, water, and surfactant in the system [3]. The figure clearly shows that our model is behaving as one would expect; the interfacial tension is reduced dramatically just by simply increasing the presence of amphiphile in the system, this being in exact accord with experiment [25]. It is worth mentioning that our results also closely mimic the interfacial behavior in a mixture of two immiscible polymers to which is added a linear diblock copolymer comprised of units of both of the immiscible polymers: a sharp decrease in interfacial tension is observed with the addition of a small amount of copolymer, which compares well with the linear section of the graph, followed by a leveling off as the copolymer concentration is increased. The leveling off at higher concentrations is indicative of interfa-

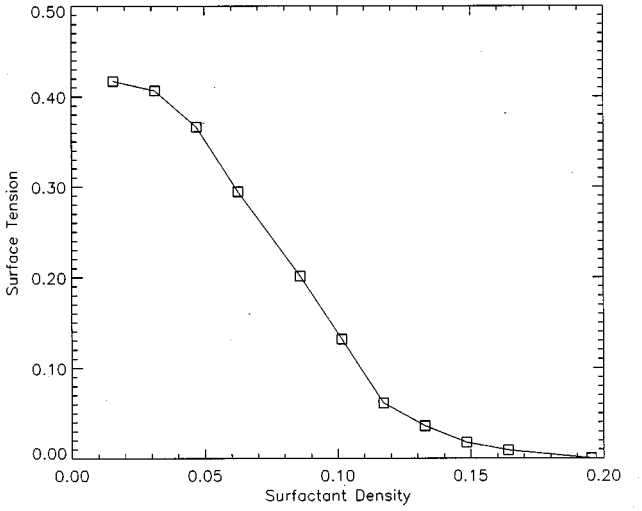

FIG. 2. Surface tension as calculated for varying amounts of amphiphile (reduced density) in the system.

cial saturation by the copolymer and subsequent formation of copolymer micelles dispersed in the homopolymer phases. The relatively flat region of the curve at very low surfactant densities is due to the tendency of a certain number of amphiphiles to exist as highly dynamic monomers within the bulk oil and water regions. As more surfactant is subsequently added to the system, these molecules preferentially align at the energetically favorable oil-water interfaces and so begin to strongly influence the interfacial tension. We find that, as the surfactant density is increased, the transient regime persists for a longer time: 1000 time steps for a surfactant density of 0.0156, 3000 time steps for 0.0469, and 13 000 time steps for 0.1172. This implies that we are moving towards a *critical* value of the surfactant density at which the flat interface will break up altogether and a smooth regime will never arise. This is first seen in our simulations with a surfactant density of ≈ 0.195; beyond this value, the computed average surface tension remains negative over the entire simulation and permanent breakup of the initially flat interface is observed. In Fig. 2 we have designated this point as corresponding to an effective surface tension of zero.

IV. PHASE SEPARATION IN BINARY IMMISCIBLE FLUIDS

In the 2D binary oil-water limit of our model we expect the domain growth exponent to be $n=\frac{2}{3}$, in line with the results of previous lattice-gas and related models. This is consistent with being in the inertial hydrodynamic regime, where the hydrodynamic length R_h is less than the domain size R, a condition forced on prior lattice-gas models [10] as a result of their inability to vary viscosity or surface tension independently of density. A benefit of our model is that we can access the other scaling regime, which has not previously been accomplished with lattice gases, where $R<R_h$, in a consistent manner. This is possible because of the presence of the inverse *temperaturelike* parameter β that we have introduced into our lattice-gas model [see Eq. (9)]. This gives us exactly the desired form of control, since we are able to alter the surface tension (and related viscosity) without having to change the density and consequently we can easily access the $R<R_h$ regime. In lowering β the collision step of the time update results in a slower phase separation mechanism acting at the interface between the two binary fluids, consequently the surface tension is reduced; however, the bulk viscosity is independent of β [22] and so this mechanism raises R_h. In this case we expect to find a growth exponent of $n=\frac{1}{2}$ since our model has full hydrodynamics with inherent fluctuations, resulting from a droplet-coalescence mechanism [29,10], in accordance with the predictions of Furakawa [30] and the molecular dynamics simulation results of Velasco and Toxvaerd [31]. We note that this high R_h regime can also be accessed by lattice-Boltzmann models and that one such model was used recently for an investigation into binary fluid spinoidal decomposition [32]. This group find $n=\frac{1}{3}$ and currently there is some controversy as to which is the *correct* exponent in this regime. However, it should be noted that these lattice-Boltzmann simulations do not include fluctuations and that this appears to be the important difference between the models; if such features are regarded as desirable, the noise has to be inserted by hand.

To analyze the domain growth quantitatively we obtain the first zero crossing of the coordinate-space pair-correlation function, which is equal to the characteristic domain size, $R(t)$. At time t following the quench, this correlation function is given by

$$C(\mathbf{r},t)=\frac{1}{V}\left\langle \sum_{\mathbf{x}} q(\mathbf{x},t)q(\mathbf{x}+\mathbf{r},t)\right\rangle \tag{14}$$

where $q(\mathbf{x},t)$ is the two-fluid (oil and water) density difference (total color charge) at each site, V is the volume, and the average is taken over an ensemble of initial conditions. Taking the angular average of $C(\mathbf{r},t)$ gives $C(r,t)$, the first zero crossing of which gives a measure of the characteristic domain size. Typically, at least five independent runs were averaged to determine the growth law for each system studied.

Setting $\alpha=1.0$ in Eq. (10) and the inverse temperaturelike parameter $\beta=0.5$, we perform a critical quench (that is, with equal amounts of oil and water in the system) on a simulation cell of size 256×256. The initial condition is random placement of the oil and water particles on the underlying lattice. The result is shown in Fig. 3, where we have used logarithmic scales so as to be able to observe any exponent in the algebraic power-law growth for the system. The domain growth exponent is clearly $n=\frac{2}{3}$, consistent with previous results obtained for the Rothman-Keller model [10] and characteristic of the regime $R>R_h$. It is worth mentioning that, as expected, we obtain this behavior for a wide range of values of β, from 0.3 upwards.

Further lowering of β and hence σ, the interfacial tension, allows us to access the $R<R_h$ regime, where typically the domain size is expected to be less than the hydrodynamic length. We do indeed observe a different scaling exponent. The result for $\beta=0.137$ is contained in Fig. 4, where the exponent is clearly $n=\frac{1}{2}$. Although not included in this figure, at later times than those shown or, alternatively, with

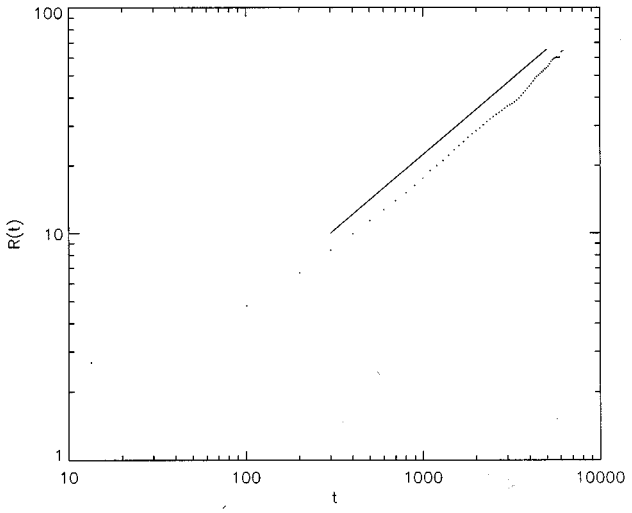

FIG. 3. Temporal (time steps) growth of domain size (lattice units), $R(t)$, for binary fluid and $\beta=0.5$, shown in a logarithmic-scale plot. The straight line has gradient 2/3 and is included as a guide only.

larger values of β, we have observed the beginnings of crossover to $t^{2/3}$ behavior, consistent with expectations. The crossover from $t^{1/2}$ to $t^{2/3}$ growth behavior occurs at a progressively earlier time as β is systematically increased from 0.137. Once β gets close to 0.3 then the $n=\frac{1}{2}$ behavior is no longer seen, the crossover effect disappears and we get $n=\frac{2}{3}$ growth right from the start of the simulations.

In order to check that the presence of the $n=\frac{1}{2}$ exponent in our results is not an artifact of incorrect dynamics in our model, we undertake two separate checks to confirm that the dynamics is indeed of type *model B* as defined by Ma *et al.* [33]; that is, there is one conserved scalar (the density) and one conserved vector (the momentum) order parameter. We

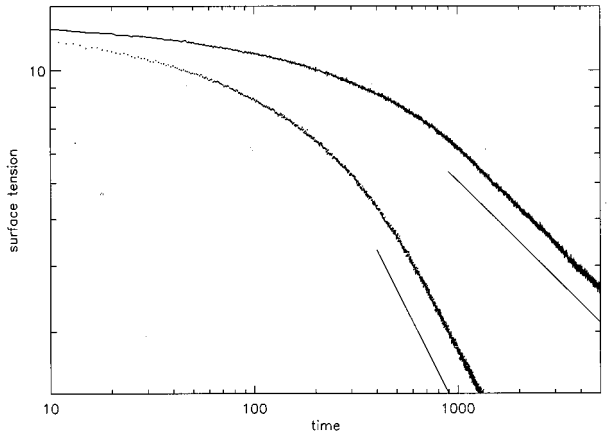

FIG. 5. Decay of surface tension with time for a binary fluid following an instantaneous change in the system to above (left-hand curve) and equal to the critical ''temperature.'' The solid lines have gradients equal to $-1/2$ (left-hand curve) and $-1/4$ and are included as a guide to the eye only.

first look at results for interface dissolution [33]. It is known that the time dependence of the decay of the interfacial tension at a binary equilibrium interface depends on whether the final ''temperature'' is above or equal to the critical temperature; we can use this knowledge to clarify the dynamics within our system. We find (see Fig. 5)

$$\sigma\sim t^{-(1/4)}, \quad \beta=\beta_c; \quad \kappa\sim t^{-1/2}, \quad \beta<\beta_c; \qquad (15)$$

these results are in exact agreement with the predictions of Ma *et al.* [33] for a *model B* binary fluid. The second check we can make is to look for the well known *model B* Liftschitz-Slyozov $t^{1/3}$ domain growth exponent in the absence of hydrodynamics. This can be accomplished by running binary fluid domain growth simulations with our model as above, but in this case we break momentum conservation

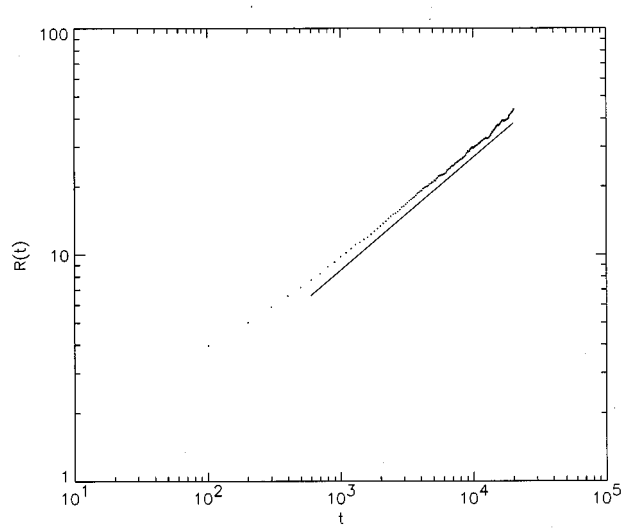

FIG. 4. Temporal (time steps) growth of domain size (lattice units), $R(t)$, for binary fluid and $\beta=0.137$, shown in a logarithmic-scale plot. The straight line has gradient 1/2 and is included as a guide only.

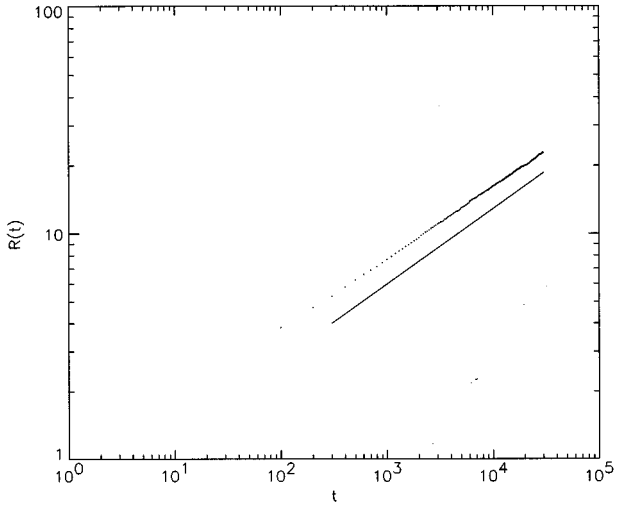

FIG. 6. Temporal growth of domain size, $R(t)$, for binary fluid with broken momentum conversation, shown in a logarithmic-scale plot. The straight line has gradient 1/3 and is included as a guide to the eye only.

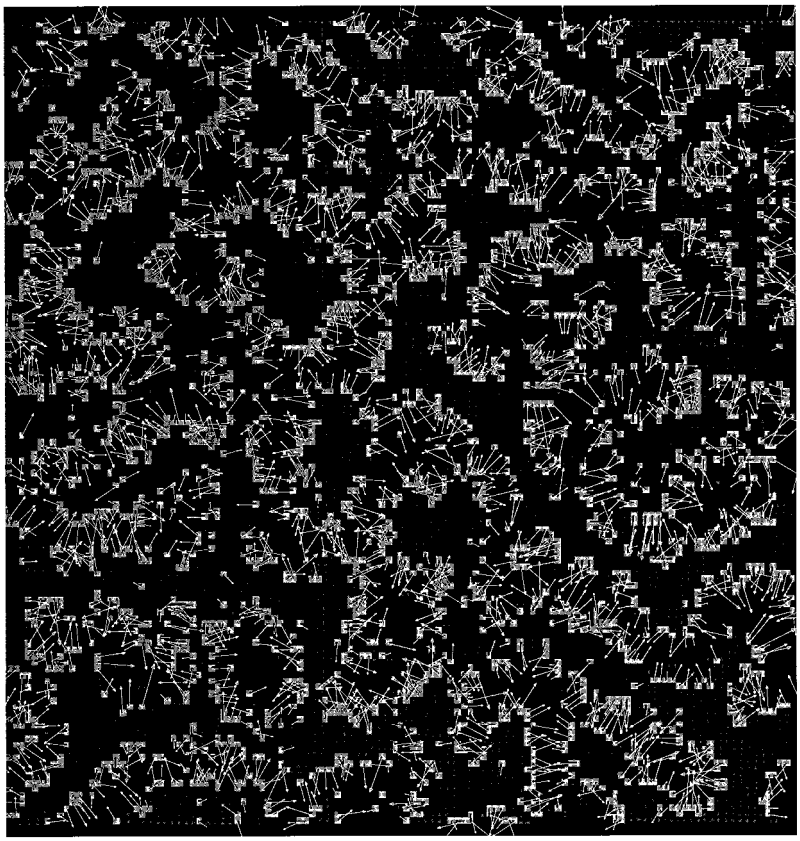

FIG. 7. Bicontinuous microemulsion structure shown at time step 200 of a simulation with equal amounts of oil and water in the system. The arrows depict the direction of the amphiphile vectors: note that they always point from the oil to water domains, as we expect.

at a predetermined percentage of sites on the lattice by reversing all particle velocities immediately after the collision process has taken place. The result is the expected $t^{1/3}$ domain growth, see Fig. 6. These results provide confirmation that the *model B* dynamics, which we are assuming to be inherent to our model, are correct.

V. SELF-ASSEMBLY KINETICS IN MICROEMULSIONS

We now turn to the analysis of the ternary system. It is clear that the presence of surfactant in an oil-water mixture dramatically alters the interfacial energetics (in particular, it lowers the interfacial tension) and so it will affect the growth of domains and consequently alter the usual binary-fluid scaling phenomena. When there is sufficient amphiphile present we expect to see some final characteristic domain size R_c imposed on the system as it reaches an equilibrium state. The effect that the amphiphile molecules have on the usual oil-water immiscible behavior is clearly shown in Fig. 7, which depicts time step 200 of a simulation of a bicontinuous microemulsion phase; the arrows show the direction and size of the color dipole vectors which represent the surfactant particles. We note that as expected the surfactant particles migrate to the oil-water interfaces and always tend to point from one color to the other, sugesting that they are exhibiting a hydrophilic-hydrophobiclike nature. Due to the immiscibility of the oil and water particles, all oil-water interfaces seek to contract in length as much as possible; the very strong requirement that the surfactant particles sit at such interfaces, however, means that at some point the shrinking must cease so the system establishes its saturated domain size. The underlying lattice-gas dynamics will of course still be present in such a system, but, by averaging over an ensemble of simulations and over time we expect to be able to determine R_c.

We begin with equal amounts of oil and water in our system while the amount of surfactant is varied for each simulation. We note that this leads to the growth of bicontinuous as opposed to droplet phases and that these are effectively equivalent to the critical quenches investigated in the binary-fluid case. Again we work with $\beta=1.0$ and use exactly the same values for the coupling coefficients in Eq. (10) as detailed earlier (in Sec. III)—consequently, all the results which follow come solely from varying the amount of surfactant in the system. In essence this consistent choice of coefficients requires the surfactant particles to sit at the bulk oil-water interfaces and discourages the formation of micelles which would hamper the accurate measure of the characteristic length scale of the bicontinuous domain. The results that follow for the ternary system have been obtained on a 128×128 lattice with periodic boundary conditions in both (x and y) directions, and with the particles initially placed on the lattice at random. The amount of surfactant used in each simulation is given in terms of its reduced density; the amount of oil and water in the system is kept constant, being at a reduced density of 0.17 for each simulation. The measurement of the domain size $R(t)$ is calculated from the spatial pair-correlation function, as described in Sec. IV.

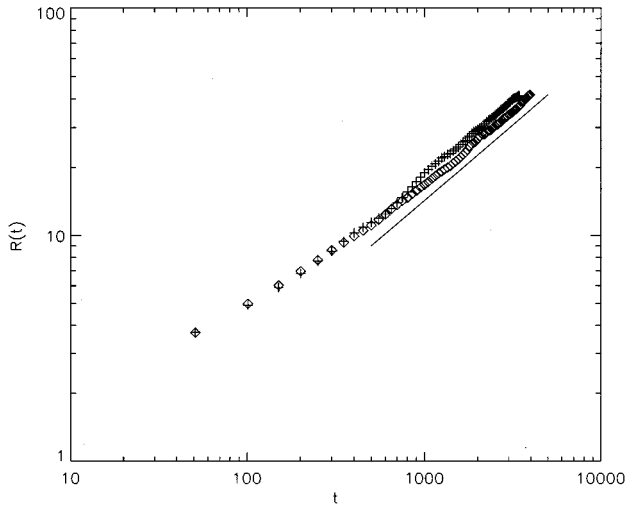

FIG. 8. Temporal (time steps) growth of domain size (lattice units), shown in a logarithmic-scale plot. The straight line has gradient 2/3 and is included as a guide to the eye. The upper symbols (crosses) are for 0.02 surfactant and the lower diamonds are for 0.04 surfactant.

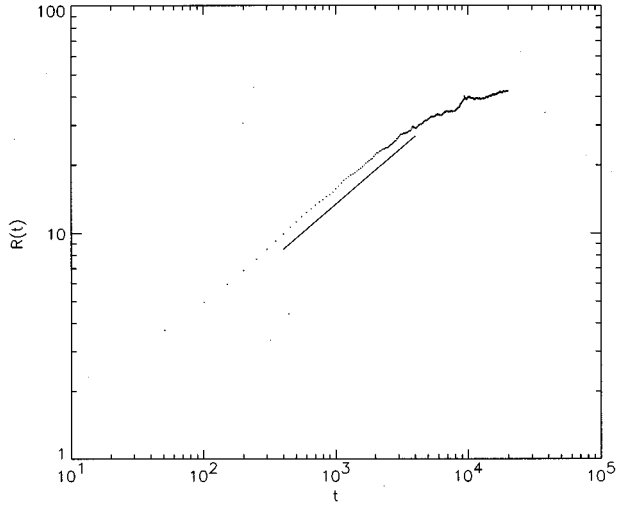

FIG. 9. Temporal (time steps) growth of domain size (lattice units), shown in a logarithmic-scale plot. The straight line has gradient 1/2 and is included as a guide to the eye. Here we have 0.06 surfactant.

The results for systems with reduced surfactant densities of 0.02 and 0.04 are shown in Fig. 8. For the former an average over five simulations is shown, while the latter consists of an average over ten. Over the late-time scaling regime, domain growth in both of these systems clearly proceeds with an algebraic exponent of $n=\frac{2}{3}$. There is insufficient amphiphile in the system to affect the oil-water binary immiscible fluid behavior. As described in Sec. III, this is consistent with the expected presence of a certain number of background amphiphilic monomers within the bulk oil and water regions, an effect which for real systems is dependent on the strength and type of amphiphile employed. If there is any change in domain growth due to the tiny amount of surfactant present in these two simulations, it would only be observed at very late times on significantly larger lattices than those we have used here. We can investigate such effects, however, by simply starting with more surfactant in the system. From our analysis in Sec. III, we expect a significant reduction in the surface tension to occur at the equivalent of a reduced density of $\simeq 0.05$ surfactant and beyond. At this point, large numbers of surfactant molecules have attached themselves to the oil-water interfaces and so begin to affect the dynamical growth of domains. Although not shown here, with a reduced density of 0.05 surfactant in the system we obtain a crossover from an exponent $n=\frac{2}{3}$ to $n=\frac{1}{2}$ at late times as surfactant molecules adsorb at the interfaces and, as expected, begin to affect the domain growth.

With reduced surfactant densities of 0.06 (and 0.07), we observe a growth exponent of $n=\frac{1}{2}$ for a majority of the time evolution, but in addition there is now a clear crossover to slower-than-algebraic growth at late times. This is depicted in Fig. 9, which contains the result for domain growth in a system with 0.06 surfactant and is obtained from an average over nine simulations, each having different initial random number seeds. The behavior described is not due to finite-size effects in the system, as we have stopped the simulations well before this becomes a problem. The observed ''jump'' of the growth exponent from $n=\frac{2}{3}$ to $n=\frac{1}{2}$, and then to slower behavior as the surfactant density is increased, is consistent with the binary-fluid behavior results that we outlined in Sec. IV. The drop in surface tension takes us into a regime that is equivalent to the slow binary one and beyond this to slower-than-algebraic growth. These results also show clear evidence of the crossover scaling transition, alluded to by Laradji *et al.* [18], from algebraic binary growth ($n=\frac{1}{2}$) to a slower domain growth when surfactants are present. Our use of a lattice-gas model, in contrast to the molecular dynamics technique employed by these authors, has the advantage of easy access to a wide range of different time-scale regimes, as the results we obtain here make evident.

Increasing the initial reduced density of amphiphile to 0.08 we see a clear departure from algebraic behavior over the time-scale of the simulations: After the first 400 time steps the slope of the curve is consistently below the line $n=\frac{1}{2}$ although the domains continue to grow over the time scale of the simulation, as shown in Fig. 10. Consequently we look at a plot of ln$t$ against domain size in order to investigate whether we now have logarithmically slow, or just slow, growth in this region. As before, this is shown plotted on logarithmic scales (see Fig. 11), so that we are able to observe any algebraic exponent for the ln$t$ growth. If the slow growth in these systems can indeed be related in some way to that in systems with quenched impurities [20], then we would expect to find some power θ for the growth function $(\ln t)^{\theta}$, which decreases as the amount of surfactant in the system is further increased. In this initial case we find a value $\theta \simeq 3.0$ for the time scale of the simulation beyond the very early-time transient behavior.

Moving to simulations with higher quantities of amphiphile, it is clear that there is enough surfactant present in the system for the domain growth to be significantly retarded. Figure 12 contains logarithmic-scale plots of $R(t)$

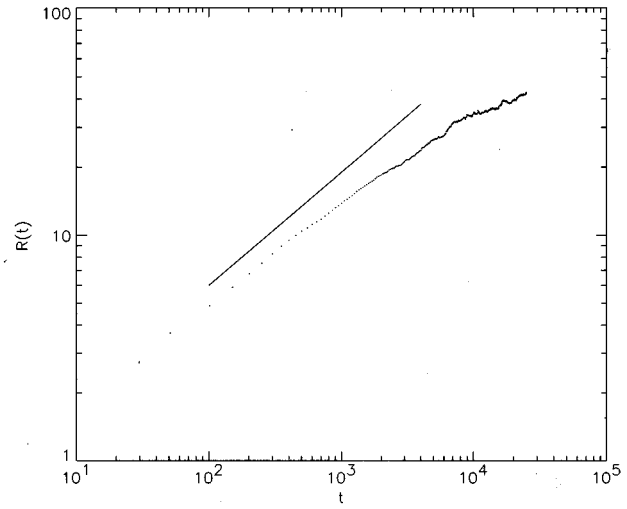

FIG. 10. Temporal (time steps) growth of domain size (lattice units), shown in a logarithmic-scale plot. The straight line has gradient 1/2 and is included as a guide to the eye. Here we have 0.08 surfactant.

versus t for 0.10 and 0.12 reduced density of surfactant, and shows that we are now in a regime where we get complete cessation of domain growth well within the finite-size limits of the system. The former of these is the result of an average over 14 runs, and the latter an average over ten. In a similar fashion to the above we reanalyze these two results, again using the logarithmic-scale plots of $R(t)$ versus ln$t$ in order to establish whether a value for the exponent θ can be extracted to help clarify the nature of the ''slow'' growth observed prior to saturation. Figure 13 contains a logarithmic-scale plot of $R(t)$ versus ln$t$ for the first of these (0.10 surfactant) and shows slow logarithmic growth with exponent $\theta \simeq 2.2$ prior to saturation. With surfactant densities of 0.12 and higher it is clear from the logarithmic-scale plots of

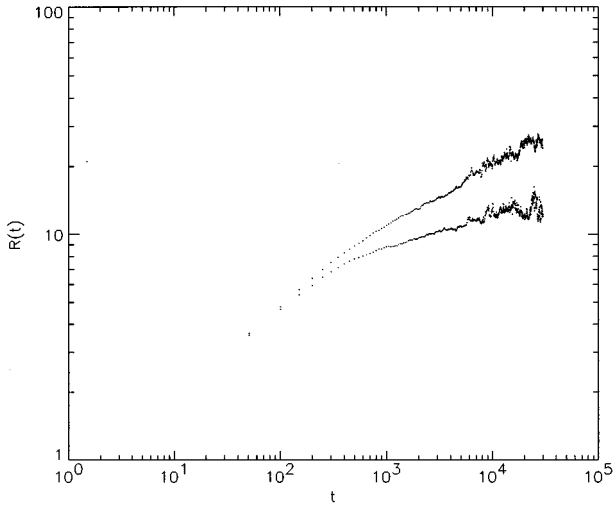

FIG. 12. Temporal (time steps) growth of domain size (lattice units), shown in a logarithmic-scale plot. The upper points correspond to 0.10 surfactant and the lower ones to 0.12 surfactant.

$R(t)$ versus t that a significant slowing down occurs after approximately the first 400 time steps of the simulations (designated as the transient region). This is obviously related to the time required for a significant proportion of the surfactant molecules present to migrate to the oil-water interfaces that form rapidly at very early times. Consequently we look at later times, although again presaturation, to establish a value for the exponent θ. Figure 14, again a logarithmic-scale plot of $R(t)$ versus ln$t$, but in this case for a surfactant density of 0.12, gives an approximate exponent of $\theta \simeq 1.1$ over the majority of the simulation running time, followed by saturation of the domain size at late times. With these intermediate surfactant densities, as clearly shown in Fig. 12, we observe large fluctuations in the measured domain size at late times in the simulations which cannot be eliminated by

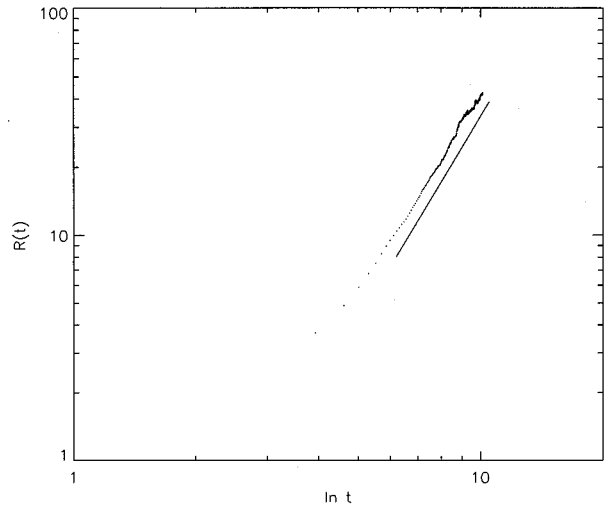

FIG. 11. Plot of ln$t$ (time steps) against growth of domain size (lattice units), shown with logarithmic scales and surfactant density of 0.08. The straight line has gradient 3.0 and is included as a guide only.

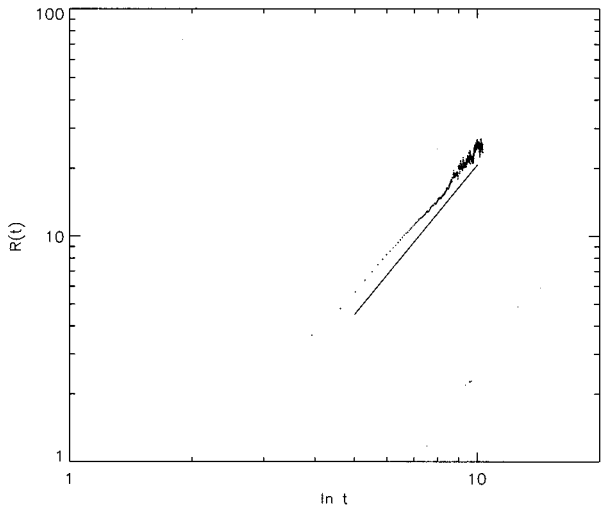

FIG. 13. Plot of domain size (lattice units) against ln$t$ (time steps), shown with logarithmic scales and surfactant density of 0.10. The straight line has gradient 2.2 and is included as a guide only.

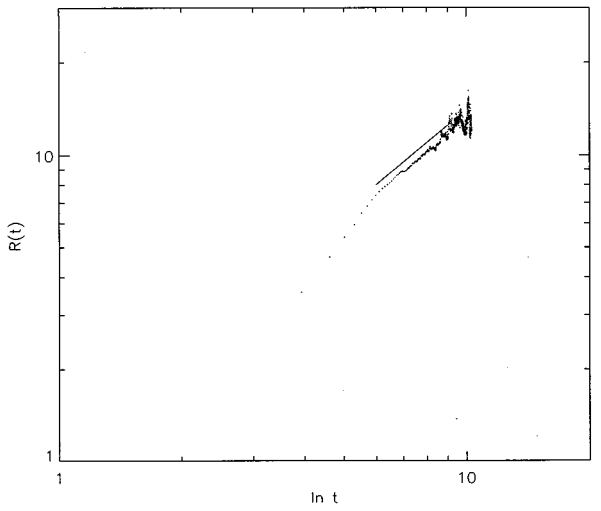

FIG. 14. Plot of domain size (lattice units) against ln$t$ (time steps), shown with logarithmic scales and surfactant density of 0.12. The straight line has gradient 1.1, and is included as a guide only.

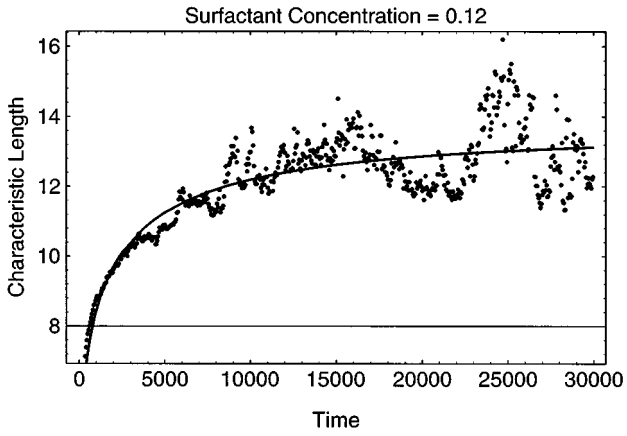

FIG. 15. Plot of domain size (lattice units) against time (time steps) for surfactant density of 0.12. The full line superimposed on the figure is the stretched-exponential fit to the data points.

ensemble averaging. Indeed, these fluctuations have an important physical basis in that they correspond to the continual break up and reformation of the bicontinuouslike structures under investigation, resulting from the finely balanced competition between the immiscible binary-fluid behavior of oil and water and the action of surfactant molecules at oil-water interfaces. As we increase the density of surfactant beyond this level, we find that the fluctuations become less severe and actually die out because sufficient surfactant molecules reside at the interfaces to effectively outweigh the oil-water interfacial tension completely. The domain structures then become strongly pinned and consequently less fluctuation is allowed by the system.

With sufficient surfactant present in the system for the domain size to reach saturation, it is clear that the logarithmic scaling is incapable of completely describing the dynamics. Consequently, following a suggestion by Douglas [34], we attempt to analyze the data in these cases in terms of a *stretched-exponential* functional form,

$$R(t)=A-B\ \exp(-Ct^{D}). \tag{16}$$

This fit has previously been successfully applied to both an experimental micellar system [35] and a simulated supermolecular spinoidal system [36] but never before has it been linked with microemulsions. Figure 15 contains the domain size against time data points and the results of the nonlinear fit to those points using the above functional form, for the case of 0.12 reduced surfactant density. The fit remains good across the full time scale of the simulation and seems to correctly describe the saturation of the system; consequently we apply this functional form as the surfactant density is further increased.

Figure 16, which contains logarithmic-scale plots of $R(t)$ versus t for simulations with relatively high amounts of amphiphile, shows that the domain growth is finally halted by the presence of sufficient surfactant: In essence we obtain a final characteristic saturated domain size for the equilibrium structures formed by the system. We expect that the average domain size will stop growing when all of the oil-water interface is covered by a surfactant ''monolayer'' [18]. Noting that the average domain size, $R(t)$, is inversely proportional to the total length of such oil-water interfaces, we then expect the final domain size to be inversely proportional to the average density of surfactants at these interfaces. However, in contrast to the deep quenches with no system fluctuations performed by Laradji *et al.* [18], where all the surfactant molecules are found at oil-water interfaces, we have a situation wherein a certain amount of the surfactant is likely to exist as monomer in bulk oil and water regions, this being confirmed by our surface tension analysis (see Sec. III). Consequently, in plotting the final domain size R_c as a function of $1/\rho_s$, where ρ_s is the average density of surfactant at the oil-water interfaces, we need to evaluate ρ_s from the total amount of surfactant in a particular system by subtracting away the ''background monomer density.'' The result is plotted in Fig. 17: We find the expected linear relationship between the final saturated domain size and the amount of interfacial surfactant in the system; that is, the final characteristic domain size is inversely proportional to the *interfacial* surfactant density in the system. The straight line on the plot is a linear fit to the first four points. (The final point, corresponding to a total reduced surfactant density of 0.09, lies below this line probably because the simulation had not fully equilibrated.) It is worth noting that the result shown in Fig. 17 is also consistent with the relationship found between the final domain size and the amplitude of disorder in systems with quenched impurities, as determined by Gyure *et al.* [20].

Although not shown here, plotting domain size versus ln$t$ for the case of surfactant density 0.14 indicates that in this case the slow domain growth may go as $(\ln t)^{\theta}$ with $\theta\simeq 0.5$ over the dominant time scale of the simulations (beyond the initial transient region) and before the domain size saturates completely. The same is true for a reduced surfactant density of 0.15, but in this case $\theta\simeq 0.3$ before saturation occurs. Table I contains a summary of how the exponent θ changes with surfactant concentration in the region of loga-

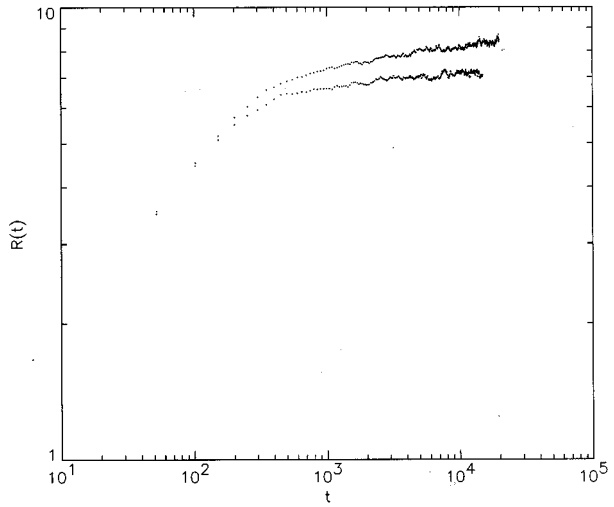

FIG. 16. Temporal (time steps) growth of domain size (lattice units), shown in a logarithmic-scale plot. Moving from top to bottom the points correspond to 0.14 and 0.15 surfactant, respectively. The upper curve is an average over ten simulations, the lower five.

rithmically slow growth studied in these and the previous simulations. These results, where the domain growth is *slow*, appear to be consistent with a picture obtained from an analysis of domain growth with quenched impurities, where the slow growth goes as $(\ln t)^{\theta}$, and where θ changes as the number of impurities is increased [20].

In addition to the logarithmic form, we have tried to fit our data sets to the stretched exponential functional form described above. The results are contained in Figs. 18 and 19. We find that the stretched-exponential form, Eq. (16), is a more accurate fit to our data than the logarithmic form, since it correctly describes the full arrest of domain growth. Of the four coefficients in this function, A is a measure of the arrested domain size, and B is uninteresting as it depends on

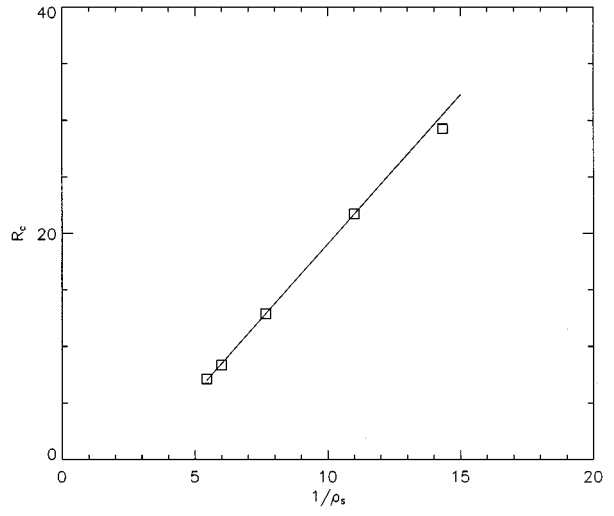

FIG. 17. Plot of the average final characteristic domain size R_c (lattice units) against the inverse of the (reduced) density of surfactant $1/\rho_s$ at the interfaces in the system.

TABLE I. Logarithmic exponent θ as it changes with surfactant concentration.

Surfactant Concentration	θ
0.08	3.0
0.10	2.2
0.12	1.1
0.14	0.5
0.15	0.3

the minimum resolvable domain size; the *decay rate* C, on the other hand, and the *stretching exponent* D are very interesting and well-behaved functions of the surfactant density. In particular, C appears to diverge as the spontaneous emulsification point is approached.

VI. DISCUSSION AND CONCLUSIONS

We have studied both binary immiscible and ternary microemulsion dynamical behavior using our hydrodynamic lattice-gas model of self-assembling amphiphilic systems. In the binary case we have found algebraic scaling laws in agreement with expectations [13], the 2D growth exponents being $\frac{1}{2}$ and $\frac{2}{3}$ at early and late times, respectively. The former is new to lattice-gas models, although it has also been observed in molecular [31], Langevin [37] and dissipative particle dynamics [38] simulations, and is also in accord with the results of a renormalization-group approach [13]. The presence of the $\frac{1}{2}$ in the former regime, as opposed to the $\frac{1}{3}$ found by lattice-Boltzmann and some other simulation techniques, appears to be as a direct result of the inclusion of natural fluctuations within the lattice-gas framework. In the ternary system we have confirmed, in accord with experiment and in a consistent manner, that the presence of surfactant results in a reduction of the oil-water interfacial tension and consequently that the growth of domains in such systems is radically different from growth in the binary case. We find a crossover from the fast $n=\frac{2}{3}$ binary regime in which we

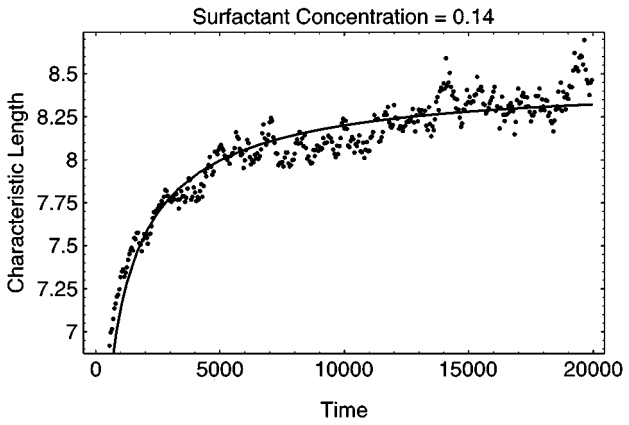

FIG. 18. Plot of domain size (lattice units) against time (time steps) for surfactant density of 0.14. The full line superimposed on the figure is the stretched-exponential fit to the data points.

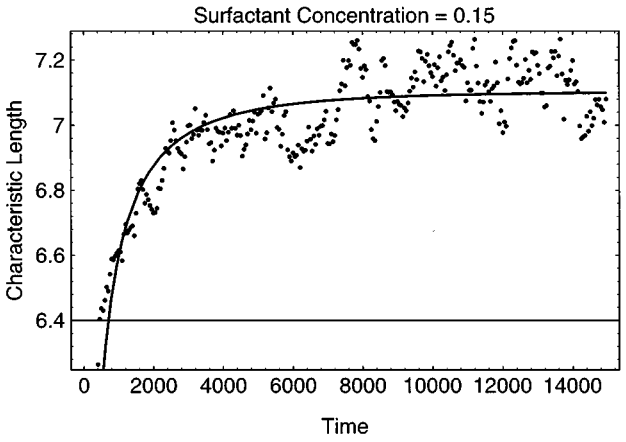

FIG. 19. Plot of domain size (lattice units) against time (time steps) for surfactant density of 0.15. The full line superimposed on the figure is the stretched-exponential fit to the data points.

begin, first to $n=\frac{1}{2}$ algebraic growth and then to ''slow'' behavior as surfactant is added to the system. This behavior mimics exactly the crossover scaling function predicted by Laradji *et al.* [18] from molecular dynamic simulations of similar systems. The greater the concentration of surfactant the slower the growth becomes; in fact, prior to saturation, it appears to be logarithmically slow, the domain size going as $(\ln t)^{\theta}$ with θ changing from 3.0 through to 0.3 as the amphiphile concentration increases through the range considered in this study. This behavior can be related to that of systems with quenched impurities in which the domains are pinned at late times, although it is not presently clear whether the apparent slow logarithmic growth behavior observed is understandable on this basis alone. In addition, we find that when the surfactant concentration is supercritical and the domain growth is arrested within the time scale of the simulation, the best *empirical* description of our system appears to be a stretched-exponential form, a result that is different for microemulsion systems of the type we are modeling here. Further work is required to establish the significance of the divergence of the coefficients of the stretched-exponential function, and, in particular, whether this has any relevance for the use of the two functional forms. In addition, detailed experimental studies of micromeulsionlike system kinetics would be useful for comparison *inter alia* with the stretched-exponential results we have obtained here.

In conclusion, we have completed an investigation into the complex dynamical behavior of the two-dimensional bicontinuous microemulsion phase, which corresponds to a critical quench in a binary oil and water system. This work represents an important extension to the validation of our recently introduced lattice-gas model for amphiphilic systems [3] as well as offering insight into the kinetics of such systems. However, our model is also able to accurately simulate off-critical droplet and micellar phases [3] and further work is required to unravel the domain growth dynamics in such situations; we expect the dynamical growth laws to be modified in some way since this is also the case for the related binary-fluid off-critical quench. Although all the simulations reported in this paper have been done in two spatial dimensions, we are currently implementing a three-dimensional version of our model [21] where again, since binary growth laws are different in three dimensions, we expect our present results to be modified.

ACKNOWLEDGMENTS

A.N.E. and P.V.C. thank Mike Swift, Julia Yeomans, Enzo Orlandini, and Giuseppe Gonella for numerous stimulating discussions. B.M.B. thanks Gene Stanley, Steve Harrington, and Francis Starr for pointing out the existence and relevance of Ref. [20], and for helpful discussions. B.M.B. also thanks Jack Douglas for numerous enlightening discussions. A.N.E. is grateful to EPSRC and Schlumberger Cambridge Research for funding his research. P.V.C. and B.M.B. are indebted to NATO for partial support for this project. B.M.B. is supported in part by Phillips Laboratory and by the United States Air Force Office of Scientific Research under Grant No. F49620-95-1-0285. B.M.B. is also grateful to the Maui High Performance Computing Center for use of their computational resources.

[1] W. M. Gelbart, D. Roux, and A. Ben-Shaul, *Modern Ideas and Problems in Amphiphilic Science* (Springer, Berlin, 1993).
[2] G. Gompper and M. Schick, Phase Transitions Crit. Phenomena **16**, 1 (1994).
[3] B. M. Boghosian, P. V. Coveney, and A. N. Emerton, Proc. R. Soc. London Ser. A **452**, 1221 (1996).
[4] A. Shinozaki and Y. Oono, Phys. Rev. Lett. **66**, 173 (1991).
[5] A. Shinozaki and Y. Oono, Phys. Rev. E **48**, 2622 (1993).
[6] A. Chakrabarti, R. Toral, and J. D. Gunton, Phys. Rev. B **39**, 4386 (1989).
[7] J. E. Farrell and O. T. Valls, Phys. Rev. B **40**, 7027 (1989).
[8] O. T. Valls and J. E. Farrell, Phys. Rev. E **47**, R36 (1993).
[9] Y. Wu, F. J. Alexander, T. Lookman, and S. -Y. Chen, Phys. Rev. Lett. **74**, 3852 (1995).
[10] S. Bastea and J. Lebowitz, Phys. Rev. E **52**, 3821 (1995).
[11] D. H. Rothman and S. Zaleski, Rev. Mod. Phys. **66**, 1417 (1994); C. Appert, J. F. Olson, D. H. Rothman, and S. Zaleski, J. Stat. Phys. **81**, 181 (1995).
[12] F. J. Alexander, S. Chen, and D. W. Grunau, Phys. Rev. B **48**, 634 (1993).
[13] A. J. Bray, Adv. Phys. **43**, 357 (1994).
[14] E. D. Siggia, Phys. Rev. A **20**, 595 (1979).
[15] T. Kawakatsu, K. Kawasaki, M. Furusaka, H. Okabayashi, and T. Kanaya, J. Chem. Phys. **99**, 8200 (1993).
[16] M. Laradji, H. Guo, M. Grant, and M. Zuckerman, J. Phys. A **24**, L629 (1991).
[17] M. Laradji, G. Hong, M. Grant, and M. Zuckerman, J. Phys. Condens. Matter **4**, 6715 (1992).
[18] M. Laradji, O. G. Mouritsen, S. Toxvaerd, and J. Zuckermann, Phys. Rev. E **50**, 1243 (1994).

[19] G. Pätzold and K. Dawson, Phys. Rev. E **52**, 6908 (1995).
[20] M. F. Gyure, S. T. Harrington, R. Strilka, and H. E. Stanley, Phys. Rev. E **52**, 4632 (1995).
[21] B. M. Boghosian, P. V. Coveney, and A. N. Emerton (unpublished).
[22] C. K. Chan and N. Y. Liang, Europhys. Lett. **13**, 495 (1990).
[23] H. Chen, S. Chen, G. D. Doolen, Y. C. Lee, and H. A. Rose, Phys. Rev. A **40**, R2850 (1989).
[24] D. H. Rothman and J. M. Keller, J. Stat. Phys. **52**, 1119 (1988).
[25] S. H. Anastasiadis, I. Gancarz, and J. T. Koberstein, Macromolecules **22**, 1449 (1989).
[26] C. Adler, D. d'Humières, and D. H. Rothman, J. Phys. (France) I **4**, 29 (1994).
[27] U. Frisch, D. d'Humières, B. Hasslacher, P. Lallemand, Y. Pomeau, and J. P. Rivet, Complex Sys. **1**, 648 (1987).
[28] J. S. Rowlinson and B. Widom, *Molecular Theory of Capillarity* (Clarendon, Oxford, 1982).
[29] M. San Miguel, M. Grant, and J. D. Gunton, Phys. Rev. A **31**, 1001 (1985).
[30] H. Furukawa, Adv. Phys. **34**, 703 (1985).
[31] E. Velasco, and S. Toxvaerd, Phys. Rev. Lett. **71**, 388 (1993).
[32] W. R. Osborne, E. Orlandini, M. R. Swift, J. M. Yeomans, and J. R. Banavar, Phys. Rev. Lett. **75**, 4031 (1995), and references therein.
[33] W.-J. Ma, P. Keblinski, J. Koplik, and J. R. Banavar, Phys. Rev. Lett. **71**, 3465 (1993).
[34] J. Douglas (private communication).
[35] J. P. Wilcoxon, J. E. Martin, and J. Odinek, Phys. Rev. Lett. **75**, 1558 (1995).
[36] S. C. Glotzer, M. F. Gyure, F. Francesco, A. Coniglio, and H. E. Stanley, Phys. Rev. E **49**, 247 (1994).
[37] T. Lookman, Y. Wu, F. J. Alexander, and S.-Y. Chen, Phys. Rev. E **53**, 5513 (1996).
[38] P. V. Coveney and K. E. Novik, Phys. Rev. E **54**, 5134 (1996).